On the Degree of Multi-Connectivity in 5G Millimeter-Wave Cellular Urban Deployments

Margarita Gapeyenko, Vitaly Petrov, Dmitri Moltchanov, Mustafa Riza Akdeniz,
Sergey Andreev, Nageen Himayat, and Yevgeni Koucheryavy

***Abstract*—Outage event caused by dynamic link blockage at millimeter-wave (mmWave) frequencies is a challenging problem for cell-edge users. To address it, 3GPP is currently working on *multi-connectivity* mechanisms that allow a user to remain connected to several mmWave access points simultaneously as well as switch between them in case its active connection drops. However, the actual number of such simultaneous links – named the *degree of multi-connectivity* – to reach the desired trade-off between the system design simplicity and the outage probability levels remains an open research question. In this work, we characterize the *outage probability* and *spectral efficiency* associated with different degrees of multi-connectivity in a typical 5G urban scenario, where the line-of-sight propagation path can be *blocked* by *buildings* as well as *humans*. These results demonstrate that the degrees of multi-connectivity of up to 4 offer higher relative gains. Our analytical framework can be further employed for the performance analysis of multi-connectivity-capable mmWave systems across their different deployment configurations.**

***Index Terms*—mmWave systems, multi-connectivity, macro diversity, dynamic human body blockage, outage probability.**

I. Introduction

The millimeter-wave (mmWave) radio links are known to be susceptible to abrupt quality degradation due to the line-of-sight (LoS) blockage by various objects in the channel including the human crowd [1], [2]. To make mmWave systems suitable for the applications that demand high reliability, 3GPP has proposed the concept of *multi-connectivity* (MC) [3].

Currently, there is a number of multi-connectivity solutions, such as dual connectivity (DC) or coordinated multi-point (CoMP) transmission/reception [4], [5]. Originally proposed in LTE Release 12, DC provides a user equipment (UE) with the radio resources of two cells residing on the same band but having different types or on multiple bands with the same cell type (multi-RAT). The multi-RAT DC for 5G is a generalization of the earlier where the UE may leverage the resources of two cells, one of which provides E-UTRA access and another one offers NR access [3]. Further, DC can be extended to multi-connectivity where the resources of two or more cells are made available to a UE. One of the MC solutions named CoMP allows to receive/transmit a signal from/to multiple cells on the same frequency [6]. It should be noted that an exact architecture for each MC option may vary and there are alternative realizations proposed [7]–[9].

Copyright (c) 2015 IEEE. Personal use of this material is permitted. However, permission to use this material for any other purposes must be obtained from the IEEE by sending a request to pubs-permissions@ieee.org.

This work was supported by Intel Corporation and the Academy of Finland (Projects WiFiUS and PRISMA). The work of V. Petrov was supported by the HPY Research Foundation funded by Elisa.

M. Gapeyenko, V. Petrov, D. Moltchanov, S. Andreev, and Y. Koucheryavy are with Tampere University of Technology, Tampere, Finland (e-mail: {firstname.lastname, evgeni.kucheryavy}@tut.fi).

M. R. Akdeniz and N. Himayat are with Intel Corporation, Santa Clara, CA, USA (e-mail: {mustafa.akdeniz, nageen.himayat}@intel.com).

The advantages of MC techniques in mmWave and microwave bands have been demonstrated in [10]–[12]. Particularly, in [11], the authors proposed a scheduling framework to distribute mmWave and microwave resources while satisfying the quality-of-service (QoS) constraints. Further, in [13], caching was employed to mitigate handover failures and reduce energy consumption at the UE side. In [14], an analysis of signal-to-interference-plus-noise ratio with MC has been contributed.

However, to satisfy high-rate constraints of the emerging applications, reliance only on microwave resources may not be sufficient. Therefore, another wave of studies related to MC was dedicated to considering multiple mmWave APs. For example, in [4], the authors employed their simulation framework to demonstrate that MC increases per-user throughput in CoMP-based scenarios, while a comparison of various AP switching strategies for MC-aided mmWave networks was targeted by [15]. In [16], an active set management scheme was proposed to avoid service interruptions.

One of the key practical aspects that has not been addressed comprehensively so far is selecting the *degree of MC*, that is, the number of simultaneously supported links. While higher degrees of MC can potentially lead to improved performance indicators and more reliable service, this also increases complexity of the networking protocols and may yield significant signaling overheads [17]. Targeting the said system design aspect, this paper analytically characterizes the outage probability and spectral efficiency in a typical outdoor urban 3GPP scenario as a function of the degree of MC with both *static* (caused by buildings) and *dynamic* (caused by humans) LoS *blockage*. We particularly focus on cell-edge users that on average experience poor channel conditions even with their closest AP.

The main contributions of this work are:

- To study the outage and spectral efficiency metrics for multi-connectivity mmWave environments in the presence of LoS blockage caused by stationary and dynamic objects, a unified mathematical framework based on stochastic geometry and probability theory is proposed.
- To evaluate relative performance benefits of higher degrees of MC, a mathematical methodology is employed. We demonstrate that the use of 4 simultaneous mmWave links allows to achieve up to 95% gain in the outage probability and up to 74% gain in the spectral efficiency, while improvements brought by higher degrees are marginal.

The remainder is organized as follows. Our system model is introduced in Section II. The outage probability and spectral efficiency for the cell-edge users in MC-aided mmWave networks are derived in Sections III and IV. Numerical results illustrating the effect of the degree of MC are offered in Section V. Conclusions are drawn in the last section.

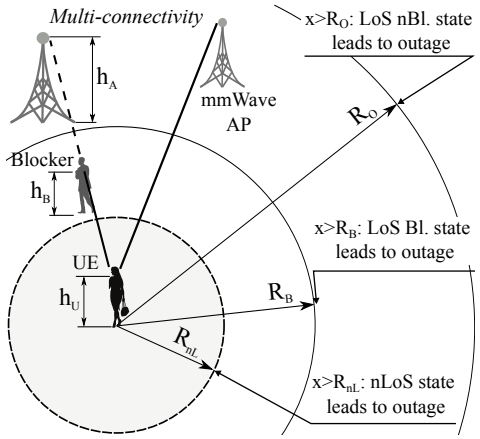

Fig. 1. Scenario considered for our analytical modeling.

II. System Model

A. Deployment Model

The system model is illustrated in Fig. 1. Assume that the locations of mmWave APs follow a Poisson point process (PPP) in $\Re^2$ with the density of λ_A. The AP height is fixed and set to h_A. We consider a single *cell-edge UE* dropped randomly in $\Re^2$, such that the distance between this UE and its nearest AP is sufficient to result in an outage; hence, the signal-to-noise ratio (SNR) is below its threshold value if the LoS link between the UE and the closest AP is blocked. The target user is assumed to remain stationary throughout its operation. The UE height, h_U, is constant as well.

The humans in the pedestrian area around the UE act as potential blockers. Their spatial density in $\Re^2$ is λ_B. These blockers are modeled as cylinders and have the radius, r_B [2]. The height of the humans is assumed constant and set to h_B, $h_B > h_U$. To capture the mmWave LoS signal dynamics, we assume that humans move according to a random direction mobility (RDM, [18]) model.

B. Propagation Model

The LoS path between a mmWave AP and a UE in dense urban environments can be blocked by: (i) large static objects, such as buildings (nLoS state), and (ii) smaller dynamic objects, such as humans (blocked state). There are four possible states for the link of interest: LoS non-blocked (nBl.) – no large or small objects are occluding the LoS link, LoS blocked (Bl.) – only small object is occluding the LoS link, nLoS non-blocked – large object is blocking the LoS, and nLoS blocked – LoS is blocked by a large object and all nLoS paths are blocked by small objects. Following the current 3GPP considerations [19], we distinguish only three of them by disregarding the worst case (nLoS blocked). The reason is that the probability that all the available independent nLoS paths are blocked simultaneously is negligible.

The LoS probability for the 2D distance x between the mmWave AP and the UE, $p_L(x)$, is obtained by using the 3GPP urban micro (UMi) street canyon model [19] as

$$p_L(x) = \begin{cases} 1, & x \leq 18 \text{ m} \\ \left(18 + xe^{-\frac{x}{36}} - 18e^{-\frac{x}{36}}\right)/x, & x > 18 \text{ m}. \end{cases} \quad (1)$$

The associated UMi path loss measured in dB for three different states (LoS nBl., LoS Bl., nLoS) is given by

$$L = \begin{cases} 32.4 + 21.0\log_{10}(d) + 20\log_{10} f_c, \text{ LoS nBl.}, \\ 52.4 + 21.0\log_{10}(d) + 20\log_{10} f_c, \text{ LoS Bl.}, \\ 32.4 + 31.9\log_{10}(d) + 20\log_{10} f_c, \text{ nLoS}, \end{cases} \quad (2)$$

where d is the three-dimensional (3D) distance between the mmWave AP and the UE, while f_c is the carrier frequency in GHz. Targeting the mean SNR value at the cell-edge, we omit the consideration of small-scale fading for simplicity.

Following the recent measurements of human body blockage effects at mmWave frequencies [1], the LoS path occlusion by humans is assumed to (on average) result in 20 dB of additional degradation in the received signal strength. Note that human body loss is a parameter and various values may be applied [20] by modifying the LoS Bl. expression in (2).

As mmWave communications employ directionality, we model directional antenna systems at both the AP and the UE sides. They are characterized by the antenna gains G_A and G_U (equal for LoS and nLoS), respectively. For simplicity, we assume cone-shaped antenna radiation patterns at both the AP and the UE, thus disregarding possible negative effects of the side lobes [21]. We also assume perfect beam alignment between the AP and UE beams in both LoS and nLoS.

C. Connectivity Model

The UE initially selects N APs with the highest received signal strength, where N is the degree of MC. We assume that the channels of a UE have been measured for sufficiently long to determine the *set* of the closest APs regardless of their instantaneous blockage situation; therefore, the static UE maintains this set of APs (e.g., a steady-state set) and does not connect to any AP beyond the N initially selected ones. The state of each selected link changes from Bl. to nBl. by following the dynamic blockage process[1] as detailed in subsection II-A. At any instant of time, the UE always chooses the best link out of N (e.g., by monitoring the received signal strength or SNR) for its data transmission, while connections over other backup links are maintained constantly via MC [9].

In our analysis, the UE first selects its closest AP in nBl. state as the one with the best SNR; in case all of the APs are blocked, it selects the closest AP in Bl. state having the SNR higher than the SNR threshold (no connection re-establishment is required when the UE selects another AP). In case all APs are blocked and/or their SNR values are below the threshold, the UE suffers from outage. Since 3GPP standardization of the MC operation is still in progress, the delay and overhead values introduced by switching between the mmWave APs are not known yet, even though they are envisioned to remain small in most scenarios [3]. In this paper, we assume idealistic switching process where the UE can instantaneously transition to its best AP out of N selected initially.

III. Multi-Connectivity Analysis

A. Outage Distance

First, let SNR at the UE be

$$S = P_A + G_A + G_U - L(f_c, d) - N_0(B), \quad (3)$$

[1]This work assumes independent blockage state changes for simplicity.

where P_A is the transmit power, G_A and G_U are the antenna gains, $L(f_c, d)$ is the path loss, while $N_0(B)$ is the total noise power at the receiver and B is the bandwidth.

We define outage as a situation, when SNR at the receiver becomes lower than a certain threshold ($S < S_T$). Hence, the minimal 2D distances between the mmWave AP and the UE resulting in outage w.r.t. the link conditions (nLoS, blocked LoS, non-blocked LoS) are given by

$$\begin{aligned} R_O &= \sqrt{10^{\frac{P_A+G_A+G_U-N_0-S_T-32.4-20\log_{10} f_c}{21}} - [h_A-h_U]^2}, \\ R_B &= \sqrt{10^{\frac{P_A+G_A+G_U-N_0-S_T-52.4-20\log_{10} f_c}{21}} - [h_A-h_U]^2}, \\ R_{nL} &= \sqrt{10^{\frac{P_A+G_A+G_U-N_0-S_T-32.4-20\log_{10} f_c}{31.9}} - [h_A-h_U]^2}, \end{aligned} \quad (4)$$

where R_O is the distance at which the link enters outage in non-blocked LoS state, R_B is the distance at which the link enters outage in blocked LoS state, R_{nL} is the distance at which the link enters outage in nLoS state, while S_T is the SNR threshold in dB. Analysis of (4) readily yields that R_O is the highest, while the relation between R_{nL} and R_B depends on the input parameters. For the sake of exposition, we further assume that $R_{nl} < R_B$ as the effect of nLoS is on average more severe than the effect of human body blockage. However, our proposed approach is generally applicable for $R_{nl} > R_B$.

B. Outage Probability

Recall that for the cell-edge users we assume no APs closer than R_{nL} to the target UE. Let A and B denote the events that there are no APs in non-outage conditions in the rings (R_{nL}, R_B) and (R_B, R_O). Denoting the outage probability for the degree of MC N by $q_{O,N}$ and using the independence property of PPP, we have $q_{O,N} = Pr(A)Pr(B)$. Consider now event A and observe that it may occur when the following two mutually exclusive events happen: (i) event A_1 of having no APs in the ring (R_{nL}, R_B) and (ii) event A_2^1 of having at least one AP in the ring (R_{nL}, R_B) jointly with the event A_2^2 of having all these APs in nLoS conditions. Let us denote the probabilities of these events by $Pr(A_1)$ and $Pr(A_2^1, A_2^2)$.

Further, event B occurs when the following mutually exclusive events happen: (i) event B_1 of having no APs in the ring (R_B, R_O), (ii) event B_2^1 of having at least one AP in the ring (R_B, R_O) jointly with event B_2^2 of having all these APs in nLoS conditions, and (iii) event B_3^1 of having the nearest $\min(N, m)$ APs in LoS blocked state jointly with the event B_3^2 of having exactly m APs in LoS conditions in the ring (R_B, R_O), and event B_3^3 of having at least one AP in that ring. We denote these probabilities by $Pr(B_1)$, $Pr(B_2^1, B_2^2)$, and $Pr(B_3^1, B_3^2, B_3^3)$. The outage probability, $q_{O,N}$, is then

$$\begin{aligned} q_{O,N} = \Big(Pr(A_1) + \big(1-Pr(A_1)\big)Pr(A_2^2|A_2^1)\Big)\Big(Pr(B_1) + \\ \big(1-Pr(B_1)\big)\big(Pr(B_2^2|B_2^1) + Pr(B_3^1, B_3^2|B_3^3)\big)\Big). \end{aligned} \quad (5)$$

Consider events A_1 and B_1. Recall that the mmWave APs follow a PPP with the density of λ_A. Hence, the probability of having no APs in the ring (R_{nL}, R_B) is offered by

$$Pr(A_1) = p_0^{R_{nL,B}} = e^{-\lambda_A \pi [R_B^2 - R_{nL}^2]}, \quad (6)$$

and, similarly, $Pr(B_1) = p_0^{R_{B,O}} = e^{-\lambda_A \pi [R_O^2 - R_B^2]}$.

To determine the probability that all of the APs in the ring (R_{nL}, R_B) are in nLoS, given that there is at least one AP in this ring, $Pr(A_2^2|A_2^1)$, we define a new process of APs that includes only those APs, which are currently in LoS. We obtain this new process as a probabilistic thinning of the original one with the probability of $p_L(x)$, thus arriving at a non-homogeneous Poisson process of APs with the density of $\lambda_A p_L(x)$, $x > R_{nL}$, which decreases along the radial lines.

The density of APs residing in LoS in (R_{nL}, R_B) is

$$\Lambda_L^{R_{nL,B}} = \frac{1}{R_B^2 - R_{nL}^2} \int_{R_{nL}}^{R_B} 2x\lambda_A p_L(x) \mathrm{d}x, \quad (7)$$

which implies that the sought probability is given by

$$Pr(A_2^2|A_2^1) = e^{-\Lambda_L^{R_{nL,B}} \pi [R_B^2 - R_{nL}^2]}. \quad (8)$$

Similarly to (8), we can obtain

$$Pr(B_2^2|B_2^1) = e^{-\Lambda_L^{R_{B,O}} \pi [R_O^2 - R_B^2]}, \quad (9)$$

where $\Lambda_L^{R_{B,O}} = \frac{1}{R_O^2 - R_B^2} \int_{R_B}^{R_O} 2x\lambda_A p_L(x) \mathrm{d}x$.

Finally, consider the probability that there are m APs residing in LoS in (R_B, R_O) and the nearest $\min(N, m)$ APs are blocked, given that there is at least one AP in this ring, $Pr(B_3^1, B_3^2|B_3^3)$. Since the UE always connects to its nearest AP, we need to have the nearest $\min(N, m)$ APs in LoS.

When there is at least one AP in LoS conditions in (R_B, R_O), we first need to obtain the distance distribution to i-th nearest AP in the ring (R_B, R_O). Let $X^{R_{B,O}}$ be the random variable (RV) denoting the distance to a randomly chosen AP in LoS conditions in (R_B, R_O) and let $f_{X^{R_{B,O}}}(x)$ be its probability density function (pdf). We thus have [22]

$$f_{X^{R_{B,O}}}(x) = \frac{x p_L(x)}{\int_{R_B}^{R_O} x p_L(x) \mathrm{d}x}. \quad (10)$$

Conditioning on m APs in the ring (R_B, R_O), the pdf of distance to the i-th nearest AP, between m independent and identically distributed (i.i.d) RVs, $Y_i^{R_{B,O}}$, becomes

$$\begin{aligned} f_{Y_i^{R_{B,O}}}(x; m) = m f_{X^{R_{B,O}}}(x) \binom{m-1}{i-1} \times \\ F_{X^{R_{B,O}}}(x)^{i-1} \Big(1 - F_{X^{R_{B,O}}}(x)\Big)^{m-i}, \end{aligned} \quad (11)$$

where $F_{X^{R_{B,O}}}(x)$ is the CDF of $X^{R_{B,O}}$ obtained from (10).

Consider the process of LoS blockage by dynamically moving blockers around a stationary user of interest and a mmWave AP located at the distance of x from the UE to concentrate on non-blockage probability. Recall that a blocker that moves according to the RDM model in a certain area is distributed uniformly in this area [18]. The probability that there is a non-blocked LoS path is then given by

$$p_{nB}(x) = e^{-2r_B \lambda_B \left[x \frac{h_B - h_U}{h_A - h_U} + r_B\right]}. \quad (13)$$

Denote by $p_{O,i}(m)$ the outage probability with i-th nearest AP in (R_B, R_O) that is currently in LoS conditions, given that there are m APs in LoS conditions in this ring. We arrive at

$$p_{O,i}(m) = \int_{R_B}^{R_O} f_{Y_i^{R_{B,O}}}(x; m) \big[1 - p_{nB}(x)\big] \mathrm{d}x, \; i \le m. \quad (14)$$

$$q_{O,N} = \left(e^{-\lambda_A \pi [R_B^2 - R_{nL}^2]} + \left(1 - e^{-\lambda_A \pi [R_B^2 - R_{nL}^2]}\right) e^{-\Lambda_L^{R_{nL,B}} \pi [R_B^2 - R_{nL}^2]} \right) \times$$
$$\left(e^{-\lambda_A \pi [R_O^2 - R_B^2]} + \left(1 - e^{-\lambda_A \pi [R_O^2 - R_B^2]}\right) \left(e^{-\Lambda_L^{R_{B,O}} \pi [R_O^2 - R_B^2]} + \sum_{m=1}^{\infty} p_m^{R_{B,O}} \prod_{i=1}^{\min(N,m)} p_{O,i}(m) \right) \right). \quad (12)$$

The probability of having m LoS APs in (R_B, R_O) is

$$p_m^{R_{B,O}} = \frac{\left(\Lambda_L^{R_{B,O}} \pi [R_O^2 - R_B^2]\right)^m}{m!} e^{-\Lambda_L^{R_{B,O}} \pi [R_O^2 - R_B^2]}. \quad (15)$$

Combining (14) and (15), the sought probability is

$$Pr(B_3^1, B_3^2 | B_3^3) = \left[1 - p_0^{R_{B,O}}\right] \sum_{m=1}^{\infty} p_m^{R_{B,O}} \prod_{i=1}^{\min(N,m)} p_{O,i}(m). \quad (16)$$

The outage probability, $q_{O,N}$, is then derived by substituting (6), (8), (9), and (16) into (5). The final result is given in (12).

IV. Spectral Efficiency

According to SNR analysis in subsection III-A, the UE is associated with j-th AP in LoS non-blocked conditions out of the nearest $\min(N, k)$ APs in the ring (R_{nL}, R_O), if $k > 0$. If there are no such APs, the UE is associated with j-th nearest AP in the ring (R_{nL}, R_B), which currently resides in LoS blocked conditions, if any. Otherwise, the spectral efficiency remains 0 until any of the APs becomes non-blocked again. Hence, spectral efficiency is a mixed RV with the probability mass at 0, the weight of $q_{O,N}$, and several "branches".

The first branch corresponds to the event of having the nearest non-blocked LoS AP with index j out of $\min(N, k)$ APs jointly with the event of having k APs residing in LoS in the ring (R_{nL}, R_O) and at least one AP in that ring. The associated probability, $q_{n,nB}$, is given by

$$q_{n,nB} = \left(1 - p_0^{R_{nL,O}}\right) \sum_{k=1}^{\infty} p_k \sum_{j=1}^{\min(N,k)} v_{j,k}, \quad (17)$$

where $p_0^{R_{nL,O}} = e^{-\lambda_A \pi [R_O^2 - R_{nL}^2]}$ is the probability of having zero APs in the ring (R_{nL}, R_O) and p_k is the probability of having k APs in LoS in the ring (R_{nL}, R_O).

The probability $v_{j,k}$ that the nearest AP in (R_{nL}, R_O) residing in nBl. LoS conditions has index $j = 1, 2, \ldots, \min(N, k)$, given that there are k APs in (R_{nL}, R_O), is

$$v_{j,k} = \left(1 - p_{B,j,k}\right) \prod_{s=1}^{j-1} p_{B,s,k}, \quad (18)$$

where $p_{B,j,k}$ is the probability of blockage at j-th nearest AP

$$p_{B,j,k} = \int_{R_{nL}}^{R_O} f_{Z_j}(x; k) \left[1 - p_{nB}(x)\right] \mathrm{d}x, \quad (19)$$

where Z_j is the RV characterizing the distance to j-th nearest AP given that there are k APs, $k \geq j$, in the ring (R_{nL}, R_O). Note that $f_{Z_j}(x; k)$ can be established similarly to $f_{Y_i}(x; m)$.

The second branch of the spectral efficiency is associated with the event of having the closest LoS AP reside in the ring (R_{nL}, R_B) jointly with the event of seeing $\min(N, k)$ LoS APs in blocked state having non-zero APs in LoS in the ring (R_{nL}, R_O). The corresponding probability, $q_{n,B}$, is given by

$$q_{n,B} = \left(1 - p_0^{R_{nL,O}}\right) \sum_{k=1}^{\infty} p_k w^{R_{nL,B}} p_{B,k} \prod_{j=2}^{\min(N,k)} p_{B,j,k}, \quad (20)$$

where $p_{B,k}$ is the probability of blockage for the closest AP in the ring (R_{nL}, R_B),

$$p_{B,k} = \int_{R_{nL}}^{R_B} f_{Z_1}(x; k) \left[1 - p_{nB}(x)\right] \mathrm{d}x, \quad (21)$$

while $f_{Z_1}(x) = k f_{X^{R_{nL,O}}}(x)(1 - F_{X^{R_{nL,O}}}(x))^{k-1}$, where $f_{X^{R_{nL,O}}}(x)$ and $F_{X^{R_{nL,O}}}(x)$ are the pdf and CDF of distance to a randomly chosen LoS AP in the ring (R_{nL}, R_O) obtained similarly to (10).

The final term in (20), $w^{R_{nL,B}}$, is the probability that the closest LoS AP resides in the ring (R_{nL}, R_B), given by

$$w^{R_{nL,B}} = \int_{R_{nL}}^{R_B} k f_{X^{R_{nL,O}}}(x) \left(1 - F_{X^{R_{nL,O}}}(x)\right)^{k-1} \mathrm{d}x. \quad (22)$$

After obtaining the probabilities for the branches of interest, the mean spectral efficiency takes the following form

$$E[C_N] = \left(1 - p_0^{R_{nL,O}}\right) \sum_{k=1}^{\infty} p_k \sum_{j=1}^{\min(N,k)} v_{j,k} \times$$
$$\int_{R_{nL}}^{R_O} f_{Z_j}(x; k) \log_2\left(1 + S_{nB,j}(x)\right) \mathrm{d}x +$$
$$\left(1 - p_0^{R_{nL,O}}\right) \sum_{k=1}^{\infty} p_k w^{R_{nL,B}} p_{B,k} \prod_{j=2}^{\min(N,k)} p_{B,j,k} \times$$
$$\int_{R_{nL}}^{R_B} f_{Z_1}(x; k) \log_2\left(1 + S_{B,1}(x)\right) \mathrm{d}x, \quad (23)$$

where $S_{nB,j}(x)$ is the SNR with j-th nearest nBl. LoS AP and $S_{B,1}(x)$ is the SNR for the first Bl. LoS AP in (R_{nL}, R_B).

V. Numerical Assessment

In this section, we numerically investigate the impact of the MC degree together with the density of blockers and APs on the outage probability and spectral efficiency. The utilized system parameters follow 3GPP and are provided in Table I. The outage thresholds, $R_{nL} = 92\,\mathrm{m}$, $R_B = 107\,\mathrm{m}$, and $R_O = 963\,\mathrm{m}$ for the SNR threshold of $S_T = 3\,\mathrm{dB}$ are computed with (2). The choice of the SNR threshold was made with a reference to services that might require high SNR levels [23]. The percentage illustrated in the plots demonstrates the difference between the metrics for the MC degree of 1 and the degree in question.

In order to verify our assumptions and analysis, we cross-check the selected analytical results against those obtained with the simulations conducted in Matlab. The geometrical deployment closely follows the procedures detailed in subsection II-A, while the channels between all of the nodes are modeled according to the 3GPP considerations [19].

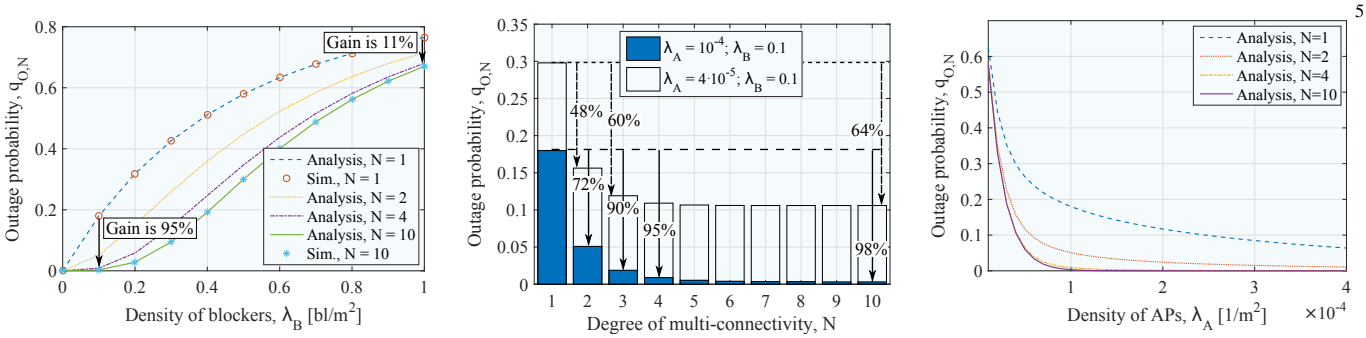

(a) Outage probability for $\lambda_A = 10^{-4}$ (b) Outage probability as function of N (c) Outage probability for $\lambda_B = 0.1$

Fig. 2. Outage probability depending on density of blockers and APs, λ_B and λ_A, and degree of multi-connectivity, N.

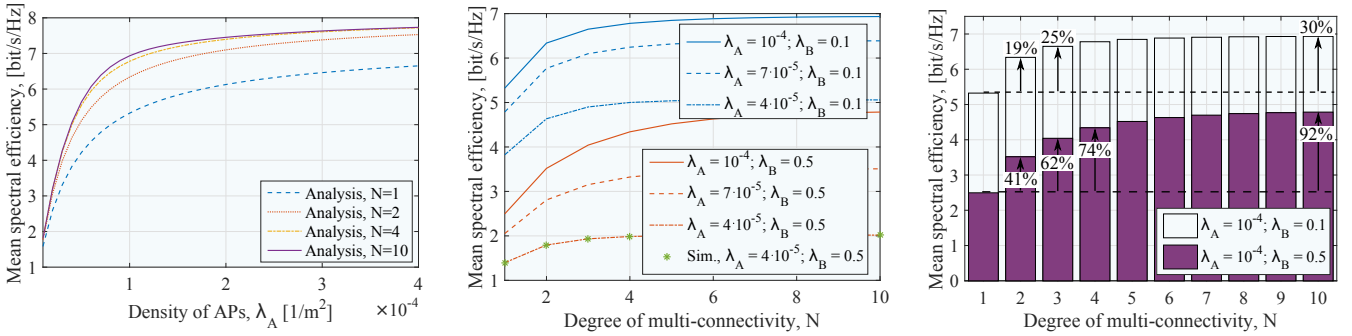

(a) Mean spectral efficiency for $\lambda_B = 0.1$ (b) Mean spectral efficiency as function of N (c) Mean spectral efficiency $\lambda_B = 10^{-4}$.

Fig. 3. Mean spectral efficiency depending on density of blockers and APs, λ_B and λ_A, and degree of multi-connectivity, N.

This framework operates in a time-driven regime with a step of 0.05 s (resulting in human movement of not more than 5 cm with the speed of 1 m/s). Each simulation round begins with a re-deployment of all the nodes of interest and then runs for 60 s of real time by reporting time-averaged performance indicators. All the intermediate simulation results have been further averaged across $1,000$ independent replications. The scenario was modeled for all the considered sets of input parameters, which demonstrated a close match between the analytical and the simulation output.

In Fig. 2(a), the outage probability is illustrated as a function of blocker density. We observe that for low densities of blockers, $\lambda_B = 0.1$, the MC degree $N = 4$ reduces the outage probability by 95% as compared to $N = 1$. However, higher densities of blockers, $\lambda_B = 1$, decrease the difference in the outage probability between the MC degrees $N = 4$ and $N = 1$ by only 11%. For the chosen system design parameters and the degree of MC, the multi-connectivity gains diminish as the density of blockers increases. The underlying reason roots in approximately geometric behavior of the probability that all the available links reside in outage conditions.

Fig. 2(b) demonstrates the impact of the MC degree on the outage probability for different AP and blocker densities $\lambda_B = 0.1$. For $\lambda_A = 10^{-4}$, adding only one additional link reduces the outage probability by 72%. Increasing the MC degree further leads to much smaller gains that vanish after $N = 4$. This is explained by the behavior of blockage probability, which tends to 1 with an increased distance between the AP and the UE. Also, decreasing the density of APs down to $\lambda_A = 4 \cdot 10^{-5}$ shrinks the difference between the two neighboring bars as compared to the same bars with $\lambda_A = 10^{-4}$. It could be explained by the fact that the APs in sparse deployments are located (on average) farther away, which leads to lower non-blockage probabilities. Moreover, the benefit of having $N = 4$ links comprises 97% of all the available gains when increasing the degree MC to ∞. Also note that increased SNR thresholds lead to a decreased number of APs, which a UE may communicate with at increased AP-UE distances. Therefore, the UE cannot exploit higher degrees of MC when the SNR threshold is high.

TABLE I
BASELINE SYSTEM PARAMETERS

Parameter	Value
Heights of AP, UE, and blockers, h_A, h_U, h_B	10 m, 1.5 m, 1.7 m, [19]
Radius of a blocker, r_B	0.25 m, [2]
Frequency and bandwidth	28 GHz and 1 GHz, [19]
Transmit power, P_A	35 dBm, [19]
Gain, Rx- and Tx-side, G_U and G_A	5 dB and 10 dB, [24], [25]
SNR threshold, S_T	3 dB, [23]

Fig. 2(c) and 3(a) highlight the effects of AP density on the outage probability and the mean spectral efficiency. As can be seen in the plot, for a lower density of APs (e.g., $\lambda_A = 10^{-5}$) the outage probability is rather low as well; moreover, the gains at higher degrees of MC are negligible. It can be explained by the fact that the distance between the closest AP and the UE is large, which makes the received signal weak (due to blockage and path loss). Farther located APs cannot deliver better signal quality, as they experience even worse channel conditions. The benefit in the increased degrees of MC is noticed for the density of APs equal to $\lambda_A = 3 \cdot 10^{-5}$ to $\lambda_A = 2 \cdot 10^{-4}$. By growing the density of APs further, the main AP offers channel conditions that are sufficient for the UE to reside on the same AP without switching to other ones.

In Fig. 3(b), the mean spectral efficiency as a function of the MC degree is shown for different values of λ_B and λ_A. As one may observe, high densities of blockers (e.g., $\lambda_B = 0.5$) can be partially compensated by denser AP deployments and higher MC degrees. With the latter parameters, the same spectral efficiency is observed at much lower blocker densities,

$\lambda_B = 0.1$, and for a sparse AP deployment $\lambda_A = 4 \cdot 10^{-5}$. Therefore, the mean spectral efficiency in highly crowded scenarios may be improved by densifying the AP deployment and enabling the MC capability. However, one should note that densification may lead to increased interference, which can require coordination. In our study, for the given AP density we assume noise-limited operation [26].

The relative MC gains for the mean spectral efficiency are further depicted in Fig. 3(c). As one may notice, the relation between the increased MC degree and the corresponding benefits follows the same trend as the outage probability assessed in Fig. 2(b). The main contributions are observed with $N = 2$ and then with $N = 3$. A further increase of the MC degree provides negligible impact. Note that $N = 2$ offers the highest relative gain of over 40% in crowded environments with higher densities of APs as compared to under 20% in low blockage scenarios with $\lambda_B = 0.1$. The latter effect is explained by already high spectral efficiency at lower densities, which is sufficiently close to its upper limit.

VI. Conclusion

Multi-connectivity is a recently introduced 3GPP consideration to improve the performance in the emerging mmWave networks. However, it is also expected to increase the complexity and signaling overheads of its enabling protocols. Hence, a careful selection of the *degree of MC* for a given deployment is of particular importance. In this work, we develop an analytical model to study the *outage probability* and the *spectral efficiency* in mmWave networks with the MC capability by capturing the key mmWave deployment, accounting for *nLoS*, *blocked*, and *non-blocked LoS* link conditions, as well as dynamic transitions between these states. Future work on this topic may include a performance study of upper-layer protocols and beamforming overheads, as well as the consideration of spatial and temporal consistency and the effect of blocker density on the attenuation, among others.

Our numerical results support the following observations:

• For a moderately dense human crowd, $\lambda_B \in [0.05; 0.7]$, the use of the MC degrees of 2–4 notably improves both outage and spectral efficiency metrics for the cell-edge users over a given range of deployment parameters. In contrast, any higher MC degree does not significantly benefit the performance, which is important to note, since a higher degree of MC may impose additional overheads on connectivity management.

• The MC technique is most beneficial at moderate densities of human blockers around the UE, $\lambda_B \in [0.05; 0.7]$. With lower values of λ_B, the environment does not benefit from reliance on the MC operation, whereas even the MC degree of 10 cannot mitigate the outage probability for ultra-dense crowds, since all of the possible paths around the UE become blocked.

References

[1] K. Haneda *et al.*, "5G 3GPP-like channel models for outdoor urban microcellular and macrocellular environments," in *IEEE 83rd Vehicular Technology Conference (VTC Spring)*, pp. 1–7, May 2016.

[2] M. Gapeyenko *et al.*, "On the temporal effects of mobile blockers in urban millimeter-wave cellular scenarios," *IEEE Transactions on Vehicular Technology*, vol. 66, pp. 10124–10138, November 2017.

[3] 3GPP, "NR; Multi-connectivity; Overall description (Release 15)," 3GPP TS 37.340 V15.2.0, June 2018.

[4] F. B. Tesema, A. Awada, I. Viering, M. Simsek, and G. P. Fettweis, "Mobility modeling and performance evaluation of multi-connectivity in 5G intra-frequency networks," in *IEEE Globecom Workshops (GC Wkshps)*, pp. 1–6, December 2015.

[5] D. Ohmann, A. Awada, I. Viering, M. Simsek, and G. P. Fettweis, "Impact of mobility on the reliability performance of 5G multi-connectivity architectures," in *IEEE Wireless Communications and Networking Conference (WCNC)*, pp. 1–6, March 2017.

[6] L. Cheng *et al.*, "Coordinated multipoint transmissions in millimeter-wave radio-over-fiber systems," *Journal of Lightwave Technology*, vol. 34, pp. 653–660, January 2016.

[7] A. Ravanshid *et al.*, "Multi-connectivity functional architectures in 5G," in *Proc. of IEEE International Conference on Communications Workshops (ICC)*, pp. 187–192, May 2016.

[8] D. S. Michalopoulos, I. Viering, and L. Du, "User-plane multi-connectivity aspects in 5G," in *Proc. of 23rd International Conference on Telecommunications (ICT)*, pp. 1–5, May 2016.

[9] M. Giordani, M. Mezzavilla, S. Rangan, and M. Zorzi, "An efficient uplink multi-connectivity scheme for 5G millimeter-wave control plane applications," *IEEE Transactions on Wireless Communications*, vol. 17, pp. 6806–6821, October 2018.

[10] M. Polese, M. Giordani, M. Mezzavilla, S. Rangan, and M. Zorzi, "Improved handover through dual connectivity in 5G mmWave mobile networks," *IEEE Journal on Selected Areas in Communications*, vol. 35, pp. 2069–2084, September 2017.

[11] O. Semiari, W. Saad, and M. Bennis, "Joint millimeter wave and microwave resources allocation in cellular networks with dual-mode base stations," *IEEE Transactions on Wireless Communications*, vol. 16, pp. 4802–4816, July 2017.

[12] V. Petrov *et al.*, "Achieving end-to-end reliability of mission-critical traffic in softwarized 5G networks," *IEEE Journal on Selected Areas in Communications*, vol. 36, pp. 485–501, March 2018.

[13] O. Semiari, W. Saad, M. Bennis, and B. Maham, "Caching meets millimeter wave communications for enhanced mobility management in 5G networks," *IEEE Transactions on Wireless Communications*, vol. 17, pp. 779–793, February 2018.

[14] D. Öhmann, A. Awada, I. Viering, M. Simsek, and G. P. Fettweis, "Achieving high availability in wireless networks by inter-frequency multi-connectivity," in *Proc. of IEEE International Conference on Communications (ICC)*, pp. 1–7, May 2016.

[15] V. Petrov *et al.*, "Dynamic multi-connectivity performance in ultra-dense urban mmwave deployments," *IEEE Journal on Selected Areas in Communications*, vol. 35, pp. 2038–2055, September 2017.

[16] F. B. Tesema, A. Awada, I. Viering, M. Simsek, and G. Fettweis, "Multiconnectivity for mobility robustness in standalone 5G ultra dense networks with intrafrequency cloud radio access," *Wireless Communications and Mobile Computing*, pp. 1–17, January 2017.

[17] F. B. Tesema, A. Awada, I. Viering, M. Simsek, and G. Fettweis, "Evaluation of context-aware mobility robustness optimization and multi-connectivity in intra-frequency 5G ultra dense networks," *IEEE Wireless Communications Letters*, vol. 5, pp. 608–611, December 2016.

[18] P. Nain, D. Towsley, B. Liu, and Z. Liu, "Properties of random direction models," in *IEEE 24th Annual Joint Conference of the IEEE Computer and Communications Societies*, vol. 3, pp. 1897–1907, March 2005.

[19] 3GPP, "Study on channel model for frequencies from 0.5 to 100 GHz (Release 15)," 3GPP TR 38.901 V15.0.0, June 2018.

[20] J. S. Lu, D. Steinbach, P. Cabrol, and P. Pietraski, "Modeling human blockers in millimeter wave radio links," *ZTE communications*, vol. 10, pp. 23–28, December 2012.

[21] V. Petrov *et al.*, "Interference and SINR in millimeter wave and terahertz communication systems with blocking and directional antennas," *IEEE Transactions on Wireless Communications*, vol. 16, pp. 1791–1808, March 2017.

[22] D. Moltchanov, "Distance distributions in random networks," *Elsevier Ad Hoc Networks*, vol. 10, pp. 1146–1166, August 2012.

[23] K. Belbase, Z. Zhang, H. Jiang, and C. Tellambura, "Coverage analysis of millimeter wave decode-and-forward networks with best relay selection," *IEEE Access*, vol. 6, pp. 22670–22683, 2018.

[24] K. Sahota, "5G mmwave radio design for mobile products," tech. rep., 5G Summit, June 2017.

[25] M. Matalatala *et al.*, "Performance evaluation of 5G millimeter-wave cellular access networks using a capacity-based network deployment tool," *Mobile Information Systems*, pp. 1–9, 2017.

[26] M. Rebato, M. Mezzavilla, S. Rangan, F. Boccardi, and M. Zorzi, "Understanding noise and interference regimes in 5G millimeter-wave cellular networks," in *22th European Wireless Conference*, May 2016.